Photogeneration and Transport of Charge Carriers in Poly(hydroxyamino esters)

A. Yu. Kryukov, A. A. Pakhratdinov, and A. V. Vannikov*

A. N. Frumkin Institute of Electrochemistry, Academy of Sciences of the USSR, Leninsky Prospekt, 31, 117071 Moscow, USSR

A. V. Anikeev and L. I. Kostenko

Institute of Physico-Organic Chemistry and Coal Chemistry, Academy of Sciences of the Ukrainian SSR, R. Luxemburg, 70, 340114 Donezk, USSR

Received May 31, 1991. Revised Manuscript Received September 20, 1991

The mechanism of photogeneration and hole transport in poly(hydroxyamino esters) (PHA) has been investigated by electrophotographic and time-of-flight methods. The spectral and electric field dependencies of photogeneration efficiency of holes in PHA films without and with addition of CBr_4 has been studied. Under the UV photolysis of PHA films containing CBr_4, the polycation product, acting as an effective sensitizer, is formed. The field dependencies of photogeneration efficiency are interpreted within the framework of the Onsager model. Superlinear thickness dependence of hole transit time fits well with dispersive non-Gaussian transport. The hole drift mobility and activation energy are equal to 2×10^{-10} $m^2/V \cdot s$ and 0.25 eV at electric field 8×10^7 V/m.

Introduction

The investigation of photochemical and electrophysical properties of linear addition polymers from aromatic amines and diepoxide[1,2] is of great interest in connection with the opportunity of working out the light- and ionizing-radiation-sensitive materials. Due to the photoconductive and good film formed properties, PHA are prospective candidates for application in electrophotography.[3-5] The introduction of halogen-containing acceptors, for example, CBr_4, in PHA films provides the opportunity to obtain some new properties and broaden the abilities of film systems on the basis of PHA. In absorption spectra of PHA films containing CBr_4, a new band in the range 300–480 nm appears which belongs to the charge-transfer complex (CTC). This CTC is formed between the electron acceptor and the electron-donor amino group.[5,6] Under the action of light or ionizing radiation the oxidation of PHA and the formation of products of the polycation nature occur.[5-11] These products possess intensive absorption in the visible region of spectrum.

Due to the presence of the acceptor and due to the possibility of photochemical or radiation chemical formation of polyion products, film systems based on PHA can be used as high-sensitive photo, electron, and X-ray resists[12,13] as well as electrorophotographic (EPG) or electroradiographic materials in which the "effect of memory" is realized.[14] Such systems permit the photochemical sensitization of EPG materials with regulated sensitivity.

For the synthesis of addition polymers which were described in cited papers,[1-14] many different primary monoamines and secondary diamines were used and only few diepoxides, basically bisphenol A diglycidyl ether. At the same time the synthesis and investigation of addition polymers containing other diethers or diesters are of interest. In the present paper the photoelectrical properties of poly(hydroxyamino esters) (PHA), based on *N,N'*-dibenzyl-4,4'-diaminodiphenylmethane and dicarboxylic acid, are discussed.

Experimental Section

The well-known method of producting PHA is the step growth addition reaction of *N,N'*-dibenzyl derivatives of arylamines to bisphenol diglycidyl ethers in a homogeneous melt of an equimolecular mixture of reagents at 100–120 °C during 10–20 h.[1,2] It was found that this method is also quite effective in the synthesis of PHA, based on cyclic dicarboxylic acid:

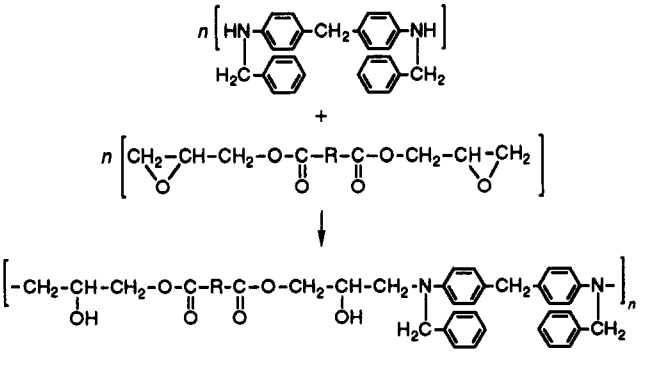

(1) Hörhold, H.-H.; Klee, J.; Bellstedt, K. *Z. Chem.* **1982**, *22*, 166.
(2) Klee, J.; Hörhold, H.-H.; Tänzer, W.; Fedtke M. *Angew. Makromol. Chem.* **1987**, *147*, 71.
(3) Opferman, J.; Horhold, H.-H.; Markiewitz, N.; Pietsch H. *J. Inf. Rec. Mater.* **1987**, *15*, 277.
(4) Stolle, Th.; Pietsch, H.; Ebert, I. *Acta Polym.* **1987**, *38*, 340.
(5) Vannikov, A. V.; Kryukov, A. Yu. *J. Inf. Rec. Mater.* **1990**, *18*, 345.
(6) Kryukov, A. Yu.; Vannikov, A. V.; Markiewitz, N. N.; Post, M. Zh. *Nauchn. Prikl. Fotogr. Kinematogr.* **1989**, *34*, 361 (in Russian).
(7) Markiewitz, N.; Pietsch, H.; Bilke, W.-D.; Post, M.; Wannikow, A. W.; Krjukow, A. Ju. *Acta Polym.* **1987**, *38*, 347.
(8) Tkachev. V. A.; Malt'zev, E. I.; Vannikov, A. V.; Kryukov, A. Yu. *Vysokomolek. Soed.* **1989**, *31* (B), 837. (in Russian).
(9) Tkachev. V. A.; Malt'zev, E. I.; Vannikov, A. V.; Kryukov, A. Yu. *Khim. Vysok. Energy* **1990**, *24*, 523 (in Russian).
(10) Kolotilkin, A. S.; Tkachev, V. A.; Malt'zev, E. I.; Vannikov, A. V.; Kryukov, A. Yu. *Khim. Vysok. Energy* **1991**, *25*, 421 (in Russian).
(11) Tkachev, V. A.; Malt'zev, E. I.; Vannikov, A. V.; Kryukov, A. Yu. *Res. Chem. Intermed.* **1990**, *13*, 7.
(12) Markiewitz, N.; Post, M.; Abraham, H. W.; Mheliss, G.; Rabe, C.; Hörhold, H.-H.; Kryukov, A.; Vannikov, A. V.; Tkachev, V. GDR Patent 277537, 1990.
(13) Kryukov, A. Yu.; Tkachev, V. A.; Vannikov, A. V.; Markiewitz, N.; Post, M.; Hörhold, H.-H. *Vysokomolek. Soed.* **1990**, *32* (B), 548 (in Russian).
(14) Kryukov, A. Yu.; Tameev, A. R.; Karasev, A. L.; Vannikov, A. V. *Zh. Nauchn. Prikl. Fotogr. Kinematogr.* **1991**, *36*, 60 (in Russian).

0897-4756/92/2804-0072$03.00/0

where

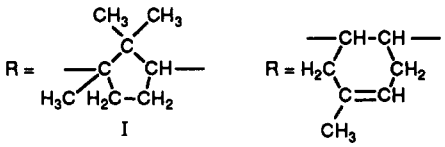

I

II

We also obtained PHA based on *N,N'*-dibenzyl-4,4'-diaminodiphenylmethane and camphoric or methyltetrahydrophthalic acids diglycidyl ester by this method. However, in the case of lower carboxylic acids this method of synthesis for PHA could not be used due to homopolymerization. Apparently the homopolymerization of lower carboxylic acids diglycidyl esters can proceed thanks to activation of hydrogen atoms of methine or methylene groups caused by the near disposition of two ester groups. For this reason, in the synthesis of PHA containing in its structure diesters of oxalic, malonic, amber, glutaric, and maleic acids, we used *N,N'*-dibenzyl-*N,N'*-bis(2,3-epoxypropil)-4,4'-diaminodiphenylmethane and the appropriate acids:

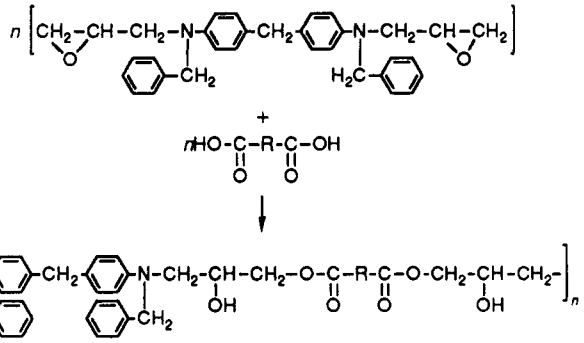

where R = H, $-CH_2-$, $-(CH_2)_2-$, $-(CH_2)_3-$, and $-CH=CH-$.

The purity of reagents and equimolecular concentration of electrophilic and nucleophilic components are important for maintaining linear multistepped additions. All analytical data were consistent with the anticipated structure.

The number-average molecular weight (M_n) has been determined by vapor pressure osmometry method. The oligomers had M_n in the range 1200–6000 and polymerization degree n in the range 2–9. In spite of the low values of M_n the films of PHA possess high physicomechanical characteristics.

Samples were prepared by dissolving PHA or mixtures of PHA and CBr_4 in $CHCl_3$. The films were then cast on Ni-coated polyethylene terephthalate or glass substrates. The thickness of the films was between 2 and 15 μm, as determined by interferometer and capacitance measurements. For time-of-flight experiments a charge generator Se layer and a semitransparent top Au electrode were deposited on the free surface. A Se layer with a thickness ~0.2 μm was situated between Au electrode and PHA film.

During a electrophotographic cycle the photoconductor film is initially charged by a corona charging device and then discharged by exposure to visible light or UV irradiation. The films were illuminated using a high-pressure Hg lamp and a MSD-1 monochromator. The surface potential could be changed with the help of the operating net. The photogeneration efficiency η was calculated using the formula

$$\eta = \frac{\Delta U \epsilon \epsilon_0 h\nu}{Le\Delta t P_\lambda (1 - 10^{-D})} \quad (1)$$

where ϵ is the dielectric constant of the film, ϵ_0 is the permittivity of free space, L is the film thickness, P_λ is the intensity of monochromatic light, D is the optical density, ΔU is the measured value of the potential drop (volts) for time Δt (seconds) upon illumination. Electrophotographic sensitivity S has been found by the formula

$$S = 1/P_\lambda \Delta t \quad (2)$$

In (1) and (2) Δt was used at which ΔU is 20% from initial surface potential. Time dependence of surface potential U is nearly linear at this time region. It is assumed that η does not change with decreasing surface potential U and applied electric field strength $F = U/L$ on 20%.

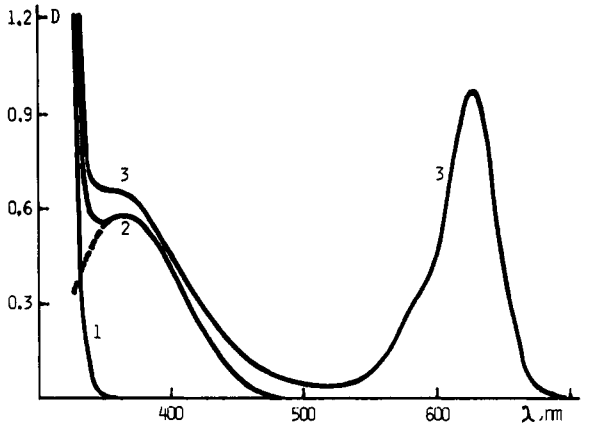

Figure 1. Absorption spectra of film II (1), film II containing CBr_4 (32 wt %) (2), and film II containing CBr_4 after UV irradiation (3). The films thickness was 6–6.5 μm. The dashed line is the difference between spectra 2 and 1.

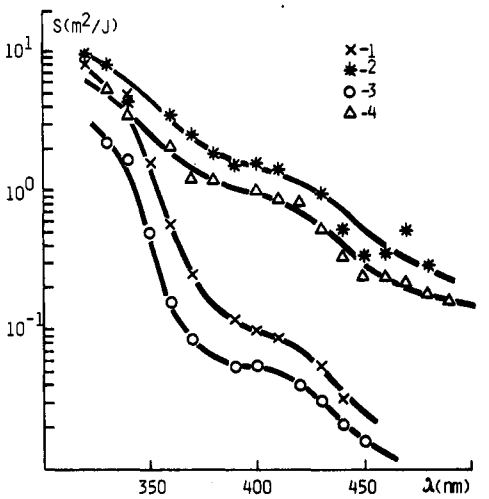

Figure 2. Spectral dependencies of electrophotographic sensitivity S for the films II (1, 2) and I (3, 4) without CBr_4 (1, 3) and with CBr_4 (32%) (2, 4). Film thickness was 6–6.5 μm; initial surface potential ~+200 V.

The drift mobility (μ) measurements were made by conventional time-of-flight technique.[15] The carriers were injected into the film by exposure to a N_2 laser (λ = 337 nm, pulse duration 10 ns). The small-signal time-of-flight regime was achieved. The transit time (t_T) of holes has been determined from transient current and μ was counted according to the formula

$$\mu = L/Ft_T \quad (3)$$

Results and Discussion

In Figure 1 the absorption spectra of films II with and without CBr_4 are shown. It is obvious from Figure 1 that with addition of acceptor the new CTC band appears in the range 340–480 nm. The basic product of photolysis of PHA is a compound of the Michler's hydrol blue type (R^+) which has absorption spectrum at λ_{max} = 630 nm (Figure 1, curve 3). The films of other PHA exhibit similar spectra.

In Figure 2 the spectral dependencies of S of the films I and II with and without CBr_4 are shown. The curves of spectral sensitivity correlate well with the absorption spectra. At λ < 360 nm the absorption spectrum is the

(15) Pfister, G.; Scher, H. *Adv. Phys.* **1978**, *27*, 747.

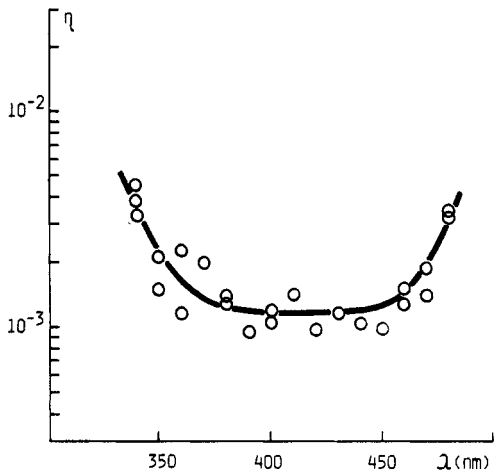

Figure 3. Spectral dependence of hole generation efficiencies η for the film II. The films thickness was 6.5 μm; initial surface potential ~+200 V.

superposition of absorption bands of PHA and CTC. With decreasing wavelength the contribution of the absorption band of PHA to the summary spectrum increases. Owing to the appearance of the additional absorption band of CTC in the near-UV and visible ranges the displacement of spectral sensitivity curve to the region of longer wavelengths for PHA film with addition of acceptor takes place. As is obvious from Figure 2 the curves for films I and II are not far from each other. The other PHA have the same values of S, i.e., the structure of diester fragments essentially does not influence the photoelectrical characteristics of PHA films.

Figure 3 shows the spectral dependence of η, which has complex shape. In the range of the mixed absorption of PHA and CTC the value of η decreases with increasing λ, i.e., with increasing contribution of CTC band to the summary absorption spectrum. The values of η in the range 360–440 nm independent of λ but at $\lambda > 440$ nm increase with increasing λ. It must be pointed out that in the range $\lambda > 360$ nm only the CTC has absorption. The increase of η with increasing λ or with decreasing the quantum energy ($h\nu$) is explained by the proceeding under the action of light of competitive processes of the charge carriers formation and photolysis.

The PHA photolysis mechanism in the presence of acceptors was investigated in detail.[8,9,11] The general scheme of photolysis is

$$(RH\cdots CBr_4) \xrightarrow{h\nu} (RH\cdots CBr_4)^* \quad (4)$$

$$(RH\cdots CBr_4)^* \rightarrow (RH^{\bullet+}\cdots CBr_4^{\bullet-}) \quad (5)$$

$$(RH^{\bullet+}\cdots CBr_4^{\bullet-}) \rightarrow R^+ + Br^- + CHBr_3 \quad (6)$$

where

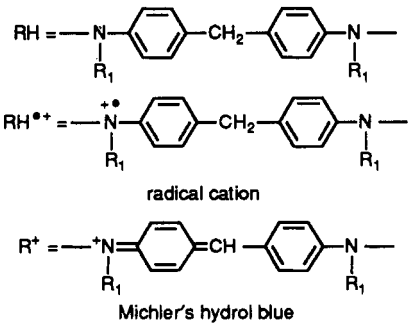

According to this scheme the transition from PHA to R^+

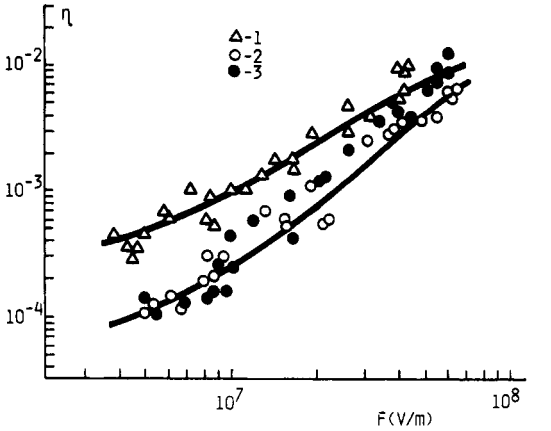

Figure 4. Field dependencies of hole-generation efficiencies η for the films II without CBr_4 (1) and with CBr_4 (32%) (2, 3) before (2) and after UV irradiation ($D_{630} = 0.85$) (3) for excitation at 380 nm. The film thickness was 6–6.5 μm. The solid curves were calculated from the Onsager equation using $\eta_0 = 0.02$, $r_0 = 35$ Å for the film II without CBr_4 and $\eta_0 = 0.04$, $r_0 = 24$ Å for the films II containing CBr_4.

occurs after light absorption by CTC (4) as a result of sequential loss of electron (5) and hydrogen atom (6) or successively proton and then electron. At light absorption by CTC the charge carriers are formed according to the reaction including dissociation of exciplex:

$$(RH\cdots CBr_4)^* \rightarrow RH^{\bullet+} + CBr_4^{\bullet-} \quad (7)$$

In refs 5, 7, and 16 it was shown that holes ($RH^{\bullet+}$) are mobile in these systems and hole transport occurs according to the reaction

$$RH + RH^{\bullet+} \rightarrow RH^{\bullet+} + RH \quad (8)$$

According to refs 17 and 18 CBr_4 and aromatic amines (Am) form the two kinds of ($Am\cdots CBr_4$) complexes in which CBr_4 is coordinated by a nitrogen atom (n–σ^* complexes) or by phenyl groups (π–σ^* complexes). The absorption spectra of the two complexes overlap; moreover, it is known the shortwave part of the CTC ($Am\cdots CBr_4$) spectrum is due to the absorption of the π–σ^* complexes while the longwave part is connected with the n–σ^* complexes. Probably excitation of the π–σ^* complexes produce ($^3Am\cdots CBr_4$) locally excited triplet states which transform into hole–electron pairs and products of photolysis (reaction 6). Excitation of the n–σ^* complexes result mainly in the formation of the hole–electron pairs.[18] That is why efficiency of the charge carriers generation in PHA increases with increasing wavelength in the longwave range.

The efficiency of the charge carriers formation at light absorption by PHA is higher than at excitation of CTC due to the proceeding of competitive process of photolysis in the latter case. At light absorption by PHA the charge carriers are formed according to the reaction

$$RH \xrightarrow{h\nu} RH^* \rightarrow RH^{\bullet+} + e \quad (9)$$

In this case photolysis, apparently, is less probable, because it goes after transfer of excitation to CTC:

$$RH^* + (RH\cdots CBr_4) \rightarrow RH + (RH\cdots CBr_4)^* \quad (10)$$

(16) Kryukov, A. Yu.; Pakhratdinov, A. A.; Khailova, E. B.; Vannikov, A. A.; Hörhold, H.-H.; Stolle, T. *Vysokomolek. Soed.* **1991**, *33* (A), 399 (in Russian).
(17) Mal'tzev, E. I.; Tkachev, V. A.; Vannikov, A. V. *J. Photochem. Photobiol. A: Chem.* **1990**, *55*, 105.
(18) Vannikov, A. V.; Grishina, A. D. *Russ. Chem. Rev.* **1989**, *58*, 1169.

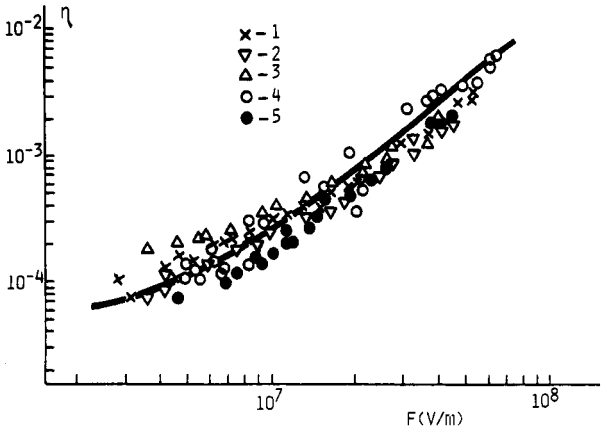

Figure 5. Field dependencies of hole generation efficiencies η for excitation at 380 nm for the films II containing CBr_4 (32%) at thickness 1.9 (1), 3.6 (2,3) 6.5 (4), and 10 μm (5) at negative (3) and positive (1, 2, 4, 5) polarities of surface potential. The solid curve was calculated from the Onsager equation with values of $\eta_0 = 0.04$ and $r_0 = 24$ Å.

In this connection with increasing λ, η increases (Figure 1, curve 3) due to the increase of part of the absorbed light by molecules PHA. The same dependence of η on λ was observed in the films of polyvinylcarbazole.[19]

In Figure 4 the dependencies of η on F at photogeneration of holes in films II by light with $\lambda = 380$ nm are shown. The field dependencies of η are described satisfactorily by the Onzager expression:[20,21]

$$\eta(r_0,F) = \eta_0\left[1 - \left(\frac{kT}{eFr_0}\right)\sum_{j=0}^{\infty} I_j\left(\frac{e^2}{4\pi\epsilon\epsilon_0 kTr_0}\right) I_j\left(\frac{eFr_0}{kT}\right)\right] \quad (11)$$

where

$$I_j(x) = I_{j-1}(x) - \frac{x^j \exp(-x)}{j!} \qquad I_0(x) = 1 - \exp(-x)$$

$$j = 1, 2, 3...$$

According to the Onsager theory, after light absorption with efficiency η_0 that does not depend on F, bound electron–hole pairs are formed. It is usually assumed that the spatial distribution of pairs is isotropic and all pairs have the same separation distance r_0. As a result of Coulomb attraction, some of these pairs recombine and the remaining pairs dissociate. Under an applied field, this dissociation process increases at the expense of the recombination process and the efficiency of the dissociation increases as well. The solid curves in Figure 4 as well as in Figures 5 and 6 are calculated from expression 11 using values $\epsilon = 3,3$ and $T = 296$ K.

It is obvious from Figure 4 that the introduction of acceptor CBr_4 leads to increasing η from 0.02 to 0.04 and at the same time to decreasing r_0 from 35 to 24 Å. The experimental points in Figure 4 for films II with and without R^+, which is acting as a sensitizer, are approximated by one and the same curve. Therefore the R^+ does not influence the process of photogeneration of charge carriers at excitation in absorption band of CTC. The value of η in films without CBr_4 is higher than in films with acceptor (Figure 4). This agrees with increasing η at increasing a part of absorbed light by molecules PHA (Figure 3). It is obvious that the increasing of η_0 at transition from PHA film without acceptor to film containing acceptor is connected with the increase of probability of charge separation due to the presence of CTC.

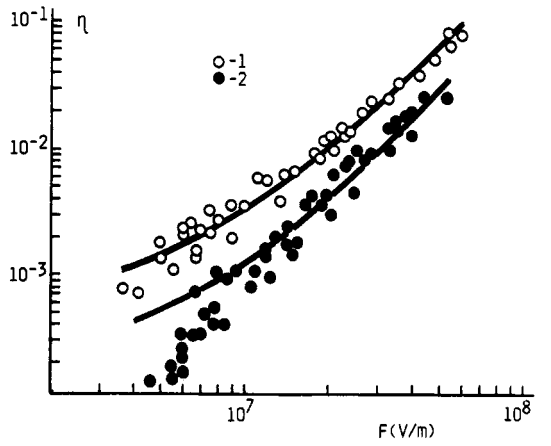

Figure 6. Field dependencies of hole-generation efficiencies η for excitation at 630 nm for the 6-μm films II containing CBr_4 (32%) and R^+ at $D_{630} = 0.02$ (1) and $D_{630} = 1.5$ (2). The solid curves were calculated from the Onsager equation using $\eta_0 = 1.00$ and $r_0 = 22$ Å for (1), and $r_0 = 19.5$ Å for (2).

Figure 5 illustrates field dependencies of η in films II at the different L and at the different polarities of the corona charge. It is seen in figure 5 that all experimental points are approximated by one curve. The absence of thickness dependence of η indicates that deep bulk traps do not influence strongly the charge carrier transport through the film. The absence of the influence of surface potential polarity on η in films with monopolar conductivity is observed under conditions of charge carrier generation in the bulk of these samples.

Figure 6 shows the field dependencies of η under illumination of films II, containing various concentrations of R^+, in maximum of absorption band of R^+ ($\lambda = 630$ nm). In this case the value of η and shapes of field dependencies of η depend greatly on the concentration of R^+. The experimental data are interpreted satisfactorily in terms of Onsager theory. The solid lines in Figure 6 are counted from eq 11. The comparison of calculated curves with experimental data shows that the value of η_0 reaches 1 at all concentrations of R^+, but r_0 decreases with increasing R^+ concentration. Earlier measurements[6,7] revealed that photodischarge of the PHA films upon illumination in absorption band of R^+ does not depend on concentration of CBr_4 and the spectral sensitivity curve is in agreement with the absorption band of sensitizer R^+. It was noted[22] that sensitizers with electron-donor substituents, after excitation, inject holes into the valence band of photoconducting polymers, for example, poly(*N*-vinylcarbazole) PVC. Thanks to the presence of electron-donor amino group in the R^+ fragment, the electron transfer between excited state of R^+ and RH after photon absorption is possible according to the following reactions:

$$R^+ \xrightarrow{h\nu} (R^+)^* \quad (12)$$

$$(R^+)^* + RH \rightarrow R^\cdot + RH^{\cdot+} \text{ (a hole)} \quad (13)$$

Apparently, CBr_4 does not influence these reactions. It can be assumed that reactions 12 and 13 can occur between the neighboring fragments of the same chain (intramolecular) as well as between fragments of different chains (intermolecular). The high concentrations of RH provide

(19) Gaidelis, V.; Montrimas, E.; Sidaravicius J. *Int. Congr. Photogr. Sci., Rochester* **1978**, 470.
(20) Melz, P. *J. Chem. Phys.* **1972**, *57*, 1694.
(21) Borsenberger P. M.; Ateya A. I. *J. Appl. Phys.* **1978**, *49*, 4035.
(22) Tani, T. *Photogr. Sci. Eng.* **1973**, *17*, 11.

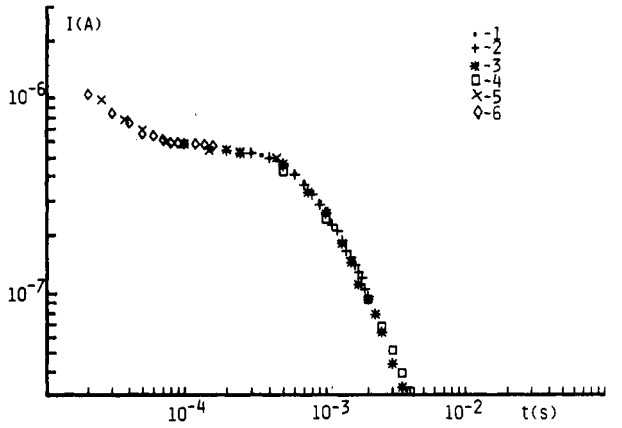

Figure 7. Transient current curve for films I at $L = 3.5$ μm, $F = 6 \times 10^7$ V/m, $T = 291$ K. Measurings at sweep 0.1 ms (1), 0.2 ms (2), 0.5 ms (3), 1.0 ms (4), 50 μs (5), and 20 μs (6).

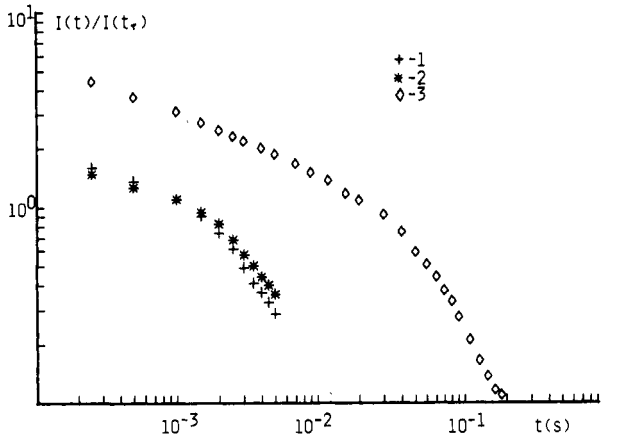

Figure 8. Transient current curves for films II without CBr_4 (1) and with 8% CBr_4 (2, 3) before (2) and after UV irradiation ($D_{630} = 0.85$) (3) at $L = 4.5$–5.5 μm, $F = 5 \times 10^7$ V/m and $T = 296$ K.

the high efficiency of formation of thermalized hole–electron pairs. It is noted that the approximate distance between neighboring diamine fragments of macromolecule of PHA ~ 20 Å, similar to magnitude of r_0. The decrease of r_0 with increasing R^+ concentration is associated with the increase in part of the intermolecular electron transfers. The departure of experimental data from Onsager curve (Figure 6, curve 2) can be explained by bulk electron–hole recombination at high concentration of R^+ ($D_{630} = 1.5$).

The shape of the current pulses in time-of-flight experiments indicates a broad dispersion of the propagating hole carrier packet. Figure 7 and 8 show transient current traces in logarithmic units recorded at the room temperature. The transient current can be described by the two distinct power law time dependencies. The t_T can be defined by intercept of the tangents approximating the current pulse at two time ranges. The transient current can be approximated by expression $I \sim t^{-(1-\alpha_1)}$ in the wide time interval at $t < t_T$ and $I \sim t^{-(1+\alpha_2)}$ at $t > t_T$, where α_1 and α_2 are the so-called dispersion parameters. The presence of CBr_4 does not influence the shape of the current pulse (Figure 8). At the same time with increasing R^+ concentration t_T increases and hence μ decreases (Figure 8). It is seen in Figure 8 that μ decreases from 5×10^{-11} to 3×10^{-12} m^2/V·s for films II owing to the availability of R^+.

The t_T for films I as for all considered earlier PHA[16] superlinearly depends on L, i.e., $t_T \sim L^{1.7}$, which testifies to dispersive (non-Gaussian) transport[15] (Figure 9). The field dependencies of t_T in logarithmic units are straight lines at high F ($F > 3 \times 10^7$V/m; Figure 9). The data for

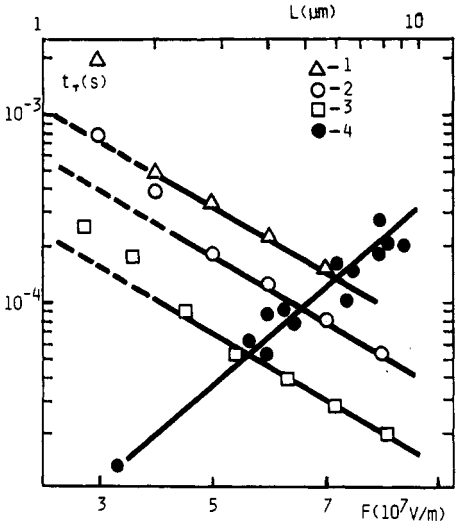

Figure 9. Field dependencies of transit time t_T for films I at thickness 8.1 μm (1), 6.5 μm (2), and 3.0 μm (3). The thickness dependence of t_T at $F = 6 \times 10^7$ V/m (4).

different L produce the straight lines which have one and the same slope. The field and thickness dependencies of t_T are in agreement with an expression well-known for the dispersive hopping transport:[15]

$$t_T \sim L^{1/\alpha} \exp(\Delta_0/kT) \exp(-e\rho F/2\alpha kT) \quad (14)$$

where ρ is the mean distance between transport sites, and Δ_0 is the activation energy at $F = 0$. With increase of F from 3×10^7 to 8×10^7 V/m the hole drift mobility increases from 4.5×10^{-11} to 2×10^{-10} m^2/V·s and activation energy decreases from 0.66 to 0.25 eV.

Conclusions

Charge carrier photogeneration and transport in photoconductive PHA films do not essentially depend on the polymer structure and have many similar features with well-studied PVC. The properties of films based on PHA and PVC have the similar magnitudes of μ, η, and S, but the PHA films have the better physicomechanichal properties than PVC films. The addition of the electron acceptors of type R-CBr_3 gives the opportunity to realize effective photochemical sensitization and to increase S in the visible region with the help of the photochemical process. Multilayer systems can be made by using the strong absorbed light. It must be pointed that CBr_4 even at high concentration (8%) does not influence upon hole transport.

The process of photogeneration of charge carriers upon excitation of CTC as well as sensitizer R^+ is satisfactorily interpreted within the framework of the Onsager theory. At the same time, the mechanisms of formation of the thermalized electron–hole pair in both cases are different. Upon excitation of the CTC, an electron is localized on the acceptor, but a hole moves and is thermalized at the distance r_0 from the electron. Excitation of R^+ causes electron transfer to occurs between the excited state of R^+ and the neighboring RH fragment. In this case the electron and the hole are at the distance r_0, which is equal to the distance between neighboring fragments R^+ and RH. The acceptor greatly influences the charge carrier photogeneration upon excitation of CTC and does not influence at the excitation of R^+. Sensitizer R^+ does not affect the charge carriers photogeneration upon excitation of CTC.

Registry No. I, 137332-67-3; II, 137393-17-0; $PhCH_2NH$-*p*-C_6H_4-CH_2-*p*-C_6H_4-$NHCH_2Ph$, 51050-64-7; -$(N(CH_2Ph)C_6H_4$-*p*-CH_2-C_6H_4-*p*-$N(CH_2Ph)CH_2CH(OH)CH_2OCOCOOCH_2CH$-

(OH)(H_2)-$_n$, 137332-68-4; -(N(CH_2Ph)C_6H_4-p-CH_2-C_6H_4-p-N(CH_2Ph)CH_2CH(OH)CH_2OCOCH_2COOCH_2CH(OH)CH_2)-$_n$, 137332-69-5; -(N(CH_2Ph)C_6H_4-p-CH_2-C_6H_4-p-N(CH_2Ph)CH_2CH(OH)CH_2OCO(CH_2)$_2$COOCH_2CH(OH)CH_2)-$_n$, 137332-70-8; -(N(CH_2Ph)C_6H_4-p-CH_2-C_6H_4-p-N(CH_2Ph)CH_2CH(OH)-CH_2OCO(CH_2)$_3$COOCH_2CH(OH)CH_2)-$_n$, 137332-71-9; -(N-(CH_2Ph)C_6H_4-p-CH_2-C_6H_4-p-N(CH_2Ph)CH_2CH(OH)-CH_2OCOCH=CHCOOCH_2CH(OH)CH_2)-$_n$, 137332-72-0; CBr_4, 558-13-4; bis(oxioyl)-1,2,2-trimethyl-1,3-cyclopentanedicarboxylate, 74567-40-1; bis(oxioyl)-4-methyl-4-cyclohexene-1,2-dicarboxylate, 137332-66-2; N,N'-dibenzyl-N,N'-bis(2,3-epoxypropil)-4,4'-diaminodiphenylmethane, 130036-13-4; oxalic acid, 144-62-7; malonic acid, 141-82-2; amber acid, 110-15-6; glutaric acid, 110-94-1; maleic acid, 110-16-7.

Surface Chemistry of Sulfidized Mercury Cadmium Telluride As Probed by Voltammetry and Photoelectrochemistry

Chang Wei, Kamal K. Mishra, and Krishnan Rajeshwar*

Department of Chemistry, Box 19065, The University of Texas at Arlington, Arlington, Texas 76019-0065

Received June 19, 1991. Revised Manuscript Received September 20, 1991

The sulfidation of mercury cadmium telluride (MCT) single crystal surfaces was studied by cyclic/linear sweep voltammetry and photoelectrochemical techniques. The study was done mainly in aqueous polysulfide solutions, although a brief comparison witn nonaqueous ethylene glycol medium is also provided, particularly with respect to oxide contamination. The evolution of the surface composition with the electrode potential was mapped by using (a) reference voltammograms for sulfidized Hg and Te surfaces along with the voltammetric behavior of polysulfide solutions at Pt, (b) linear sweep photovoltammetry, combining wavelength-selective light excitation with voltammetric scanning of the MCT surface in polysulfide, and (c) photocurrent spectroscopy (i_{ph} vs λ) at selected potentials. With these data as a unit, it is shown that CdS forms first on sulfidation of MCT followed by HgS in two stages. Subsequently, the polysulfide solution undergoes oxidation to elemental sulfur at the MCT surface along with partial oxidation of Hg to HgO (the latter only in aqueous media). At higher potentials, HgS dissolves as HgS_2^{2-}, and Te sulfidizes to TeS_2 followed by its dissolution as TeS_3^{2-}. The last stage (again only in aqueous media) comprises the generation of higher oxidation states of Te^{4+} (as TeO_x) and S^0. At positive potentials, the net result of the sulfidation is the formation of Cd-rich MCT (contrasting with the starting composition, $Hg_{0.8}Cd_{0.2}Te$). Supportive data from X-ray photoelectron spectroscopy and differential scanning calorimetry are also presented.

Introduction

Mercury cadmium telluride (MCT, $Hg_{1-x}Cd_xTe$, $x \simeq 0.2$–0.3) is a key material component of infrared systems research and technology. Since its electrical properties are dominated by surface recombination velocity, much attention has focused in recent years on strategies for passivating the surface. Anodic sulfidation of MCT has been proposed as a second-generation passivation tool by Nemirovsky and co-workers.[1-3] The earlier contention by these authors that the sulfidized surface comprised predominantly CdS has not been borne out by later studies[4,5] which have shown the presence also of significant quantities of S, Hg, and Te at the surface. The sulfidation has been carried out (predominantly by galvanostatic methods) both in nonaqueous solvents (ethylene glycol)[1-5] and in aqueous media.[6] Differences have been reported in the type of surface layers that are formed in the two cases.[6]

In spite of the fact that an electrochemical technique is employed for the sulfidation of MCT, systematic characterization of the resultant surfaces using voltammetry has not been performed. In previous studies in this laboratory,[7,10] we have shown how the information content of this powerful analytical tool is considerably enhanced by combining it with light excitation especially for photoresponsive electrode materials such as semiconductors. Thus, the primary objective of this report is to describe the voltammetric and photoelectrochemical characterization of MCT surfaces in polysulfide solutions. To probe the evolution of the surface chemistry as a function of potential, we employed a potentiostatic analysis mode, contrasting with the earlier studies.[1-6] We show that CdS forms first on the MCT surface followed by the sulfidation of the Hg and Te components at higher potentials. Finally, the dissolution of Hg and Te sulfides leaves a Cd-rich MCT surface. A brief comparison of the surface chemistry, particularly from the point of view of oxide contamination, was also performed for aqueous vs nonaqueous sulfidation media.

Experimental Section

Electrodes and Chemicals. Single crystals of MCT of nominal composition, $Hg_{0.8}Cd_{0.2}Te$, were donated by Texas Instruments, Inc. These crystals were n-type with a carrier concentration of $\sim 10^{15}$ cm^{-3}. Indium was used as the ohmic contact, and a Cu

* Author for correspondence.

(1) Nemirovsky, Y.; Burstein, L. *Appl. Phys. Lett.* **1984**, *44*, 443.
(2) Nemirovsky, Y.; Burstein, L.; Kidron, I. *J. Appl. Phys.* **1985**, *58*, 366.
(3) Nemirovsky, Y.; Adar, R.; Kornfield, A.; Kidron, I. *J. Vac. Sci. Technol.* **1986**, *A4*, 1986.
(4) Strong, R. L.; Luttmer, J. D.; Little, D. D.; Teherani, T. H.; Helms, C. R. *J. Vac. Sci. Technol.* **1987**, *A5*, 3207.
(5) Ippõshi, I.; Takita, K.; Murakami, K.; Masuda, K.; Kudo, H.; Seki, S. *J. Appl. Phys.* **1988**, *63*, 132.
(6) Ziegler, J. P.; Lindquist, J. M.; Hemminger, J. C. *J. Vac. Sci. Technol.* **1989**, *A7*, 469.
(7) Mishra, K. K.; Rajeshwar, K. *J. Electroanal. Chem.* **1989**, *271*, 279.
(8) Mishra, K. K.; Rajeshwar, K. *J. Electroanal. Chem.* **1989**, *273*, 169.
(9) Ham, D.; Mishra, K. K.; Weiss, A.; Rajeshwar, K. *Chem. Mater.* **1989**, *1*, 619.
(10) Rajeshwar, K. *Adv. Mater.*, in press.

0897-4756/92/2804-0077$03.00/0